Journal of Sound and Vibration (2000) **229**(1), 65–87
Article No. jsvi.1999.2479, available online at http://www.idealibrary.com on IDEAL®

SIMULATION OF FIRST AND SECOND ORDER SCATTERING BY ROUGH SURFACES WITH A SOUND RAY FORMALISM

J. J. EMBRECHTS

*University of Liège, Department of Applied Acoustics, Sart-Tilman B*28, *B*-4000 *Liège, Belgium*

(*Received* 19 *February* 1999, *and in final form* 16 *June* 1999)

The sound ray technique is developed to simulate rough surfaces scattering processes which are consistent with the Kirchhoff approximation (KA) theory. It is first proved that both approaches (KA and sound rays) lead to the same theoretical expression of the first-order scattered intensity. An algorithm based on the random generation of surfaces' slopes is proposed, together with some results computed for Gaussian rough surfaces. This algorithm could be used in room acoustics more as a physical substitute for the cosine Lambert law of diffusion. The method is then extended to the analysis of second-order scattering effects, which are not taken into account by KA. This new approach does not require the generation of several profiles of rough surface. However, some assumptions must be made in order to derive a useful mathematical expression of the second-order scattered intensity. The first results obtained are fairly consistent with the present knowledge of multiple scattering effects (e.g., enhanced backscattering for very rough surfaces), but further work is needed to test the assumptions and to improve the method.

1. INTRODUCTION

Taking sound scattering by rough surfaces into consideration, for example in room acoustics, often leads to the question of the angular distribution of the scattered energy. This is particularly the case when ray acoustics is used to simulate sound propagation and scattering. This problem is usually solved assuming that the rough surface acts as a uniform diffuser, and that the cosine or Lambert law can be applied to represent the angular distribution of the scattered intensity, as suggested by Kuttruff [1, 2], Hodgson [3] and Lam [4]. In reference [2], Kuttruff also analyzes the effects of different diffuse-reflection laws on the resulting sound field.

It would be interesting however to search for more "physical" solutions, i.e., solutions which are more consistent with physical theories of the sound scattering by rough surfaces. The theory which seems most suitable for this purpose is the Kirchhoff approximation (KA), since it has some connection with geometrical acoustics and, in particular, ray acoustics. Therefore, it would be interesting to implement the sound ray technique in such a way that the (simulated) scattering processes are consistent with the KA theory.

0022-460X/00/010065 + 23 $35.00/0

The KA has been developed and applied by many authors (see among others references [5–9]) to analyze the scattering of waves by significantly rough surfaces which have a small local radius of curvature. An important property of this approach is that it leads to a simple and intuitive analytical solution to the problem of scattering, which is not the case for more general numerical and/or iterative solutions of the Helmholtz integral equation [9]. The KA will be briefly reviewed in the next section. In particular, it will be seen that this theory does not necessarily require the generation of several surface profiles (by Monte Carlo methods) to derive the solution, but that only some specific statistical roughness parameters are needed.

If the distribution of the scattered energy is known by KA, then a sound ray algorithm can be based on the following principle: A given incident ray is reflected in a scattering direction defined by azimuth and polar angles, which are themselves derived from two random numbers in such a way that both angles are distributed according to the scattered intensity distribution [1, 3, 4]. This random process is more or less difficult and time-consuming, depending on the complexity of the analytical description of the scattered intensity angular distribution. Unfortunately, it turns out that mathematical expressions derived by the KA theory can be quite complicated.

Another technique is proposed in this paper. O'Donnell and Mendez [10] have already mentioned that there is a more natural relationship between KA and ray statistics, provided that KA is developed in the limiting case of geometrical acoustics ($\lambda \sim 0$). The KA theory can be developed for non-geometrical acoustics conditions [9, 11], but the limiting case ($\lambda \sim 0$) is interesting since it is closely related to the existence of the sound ray concept. O'Donnell and Mendez refer to the book of Bass and Fuks [6] who have shown, in the discussion of their equation (20.18), that the intensity scattered in a given direction is proportional to the probability that the surface slope is equal to the slope producing a specular reflection in this direction.

Going back to the problem of the sound ray algorithm, the scattering direction of the sound ray could be given by the slope at the incidence point, which would itself be derived from a random process associated with the statistical slope distribution. This technique for the scattering of sound rays seems, in a sense, more physical, and it could possibly lead to more efficient algorithms. But the random process must still be defined.

In this paper, it is first intended to describe the random generation of the slope, and to prove that the resulting sound ray algorithm effectively leads to the same distributions of scattered intensities as those predicted by the KA theory. Macaskill [12] has already shown this equivalence for some specific Gaussian rough surfaces. This author generated several profiles representative of the same statistical class of two-dimensional (2-D) (cylindrical) surfaces, and he discussed the results of a ray tracing algorithm on these profiles. He obtained average distributions of the scattered energy that were consistent with KA theory ($\lambda \sim 0$) for this particular class of surfaces. In this paper, the equivalence between KA and a sound ray algorithm will be established for any class of random 3-D rough surfaces, and the influence of the statistical roughness parameters will be investigated. Second,

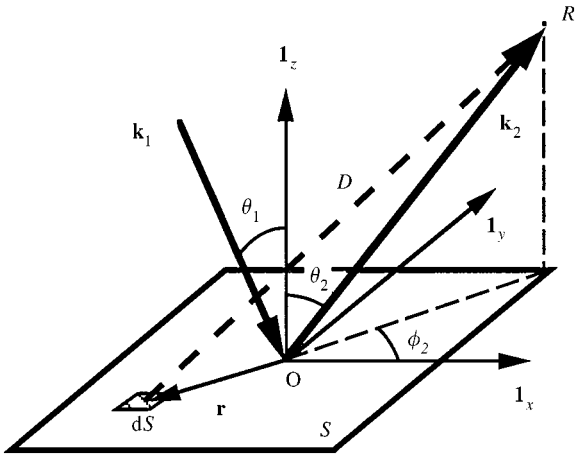

Figure 1. Scattering geometry: $\mathbf{k}_1$ is the incident wave vector in the vertical plane ($y = 0$). The angle of incidence is θ_1 and the scattering direction **OR** is defined by the angles θ_2 and ϕ_2. The mean plane of the corrugations of the rough surface is the plane ($z = 0$). Other symbols are defined in the text.

whether this technique can be extended to derive an analytical solution for second-order scattering effects will be examined.

2. THE KIRCHHOFF APPROXIMATION (KA)

Consider a plane wave, propagating along the wave vector $\mathbf{k}_1$ and incident upon a finite rough surface S (see Figure 1). The scattered wave is expressed by the sound pressure $p_s(R)$ that it produces at point R, situated a great distance away from the surface (in the Fraunhofer zone), in the direction of the wave vector $\mathbf{k}_2$:

$$p_s(\mathbf{R}) = \frac{1}{4\pi}\int_S \left(p(\mathbf{r})\frac{\partial G}{\partial n} - G\frac{\partial p(\mathbf{r})}{\partial n}\right) \mathrm{d}S,$$

$$G = \frac{1}{D}\,\mathrm{e}^{\mathrm{i}kD}, \qquad D = |\mathbf{OR} - \mathbf{r}|. \tag{1}$$

This expression is derived from the Green theorem [5], in which $p(\mathbf{r})$ is the sound pressure (incident + scattered) at the surface element $\mathrm{d}S$ (position vector $\mathbf{r}$), G is the Green function and $\partial/\partial n$ represents the derivative along the outward normal to the rough surface at $\mathrm{d}S$.

The Kirchhoff' or tangent-plane approximation consists of assuming that the pressure and its gradient can be estimated by their value at $\mathbf{r}$ as if the rough surface was locally replaced by a (infinite) tangent plane. This leads to the following expression:

$$4\pi p_s(\mathbf{R}) = \int_S \left(p_{inc}(\mathbf{r})\frac{\partial G}{\partial n} - G\frac{\partial p_{inc}(\mathbf{r})}{\partial n}\right) \mathrm{d}S + \int_S C_r(\mathbf{r}) \left(p_{inc}(\mathbf{r})\frac{\partial G}{\partial n} + G\frac{\partial p_{inc}(\mathbf{r})}{\partial n}\right) \mathrm{d}S. \tag{2}$$

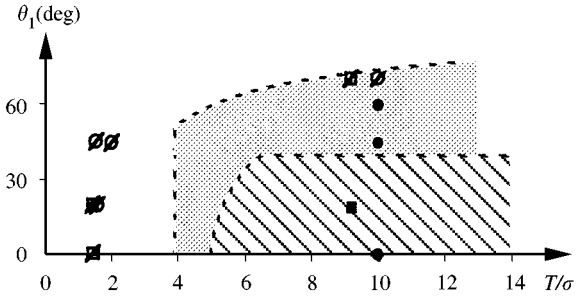

Figure 2. Approximate domain of validity of KA in the space of variables θ_1 (the angle of incidence) and T/σ (a roughness parameter defined in equation (4)). The hatched area corresponds to the domain of validity proposed by Soto Crespo *et al.* [16], while the dotted area corresponds to the domain where KA is accurate following Thorsos [9] (an additional condition formulated by Thorsos is that the observation angle must fulfill $|\cot \theta_2| < 1{\cdot}4\ T/\sigma$). Filled squares correspond to results obtained by O'Donnell and Mendez [10], for which KA is accurate, while barred squares identity results for which KA is not valid. Filled and barred circles have the same significance for results obtained by Macaskill and Kachoyan [17].

The reflection coefficient $C_r(\mathbf{r})$ depends moreover on the local angle of incidence θ_i on the rough surface at $\mathbf{r}$. The first integral term of equation (2) would correspond to the scattering pressure created by a surface characterized by $C_r = 0$. Therefore, it is not significant and can be omitted. This term leads in fact to edge effects created by the finite size of the rough surface, which become negligible when this size is much greater than the wavelength (see reference [8]).

It is difficult even today to precisely formulate the KA conditions of validity. It can be considered that the local radius of curvature of the rough surface must be "much greater" than the ratio of the wavelength to the factor $(\cos^3 \theta_i)$: see, for example, Bass and Fuks [6] or McDaniel and Gorman [13]. This consideration implies that the KA can pose problems at grazing incidence, and this is reinforced by the fact that equation (2) does not account for shadowing and multiple scattering between the surface elements dS. For statistically rough surfaces, the conditions of validity found in the literature often refer to the angle of incidence (θ_1 in Figure 1), the r.m.s. slope and the ratio T/λ between the correlation length and the wavelength: KA is valid if this ratio is greater than one [9, 14, 15]. Then, the KA domain of validity can be sketched as in Figure 2, which has been derived from results published in references [9, 10, 12, 16, 17].

More accurate methods and approximations to the problem of rough surface scattering have been recently developed (small-slope approximation [18, 19], operator expansion method [20]), but they are presently not in a suitable form to be introduced in a room acoustics program to take walls' diffusion into account. Moreover, they all reduce to KA at high frequencies where ray acoustics is valid. Therefore, these more recent methods will not be considered in this paper.

Bass and Fuks [6] have developed further the second integral term of equation (2) for a rough surface that is described by the equation $z = \xi(x, y)$, where ξ is a random variable. The scattered pressure $p_s(\mathbf{R})$ is itself a random variable, since it depends on ξ. It is shown that the statistical average of $p_s(\mathbf{R})$ is only significant in the specular direction.

The mean scattered intensity has two contributions. The first one is the coherent intensity, resulting from the constructive interferences of the reflected pressure waves emerging from all surface elements. This term is only significant for slightly rough surfaces (in the specular direction) and is responsible for the creation of an image of the source "below" the surface. The second contribution is the incoherent intensity, resulting from the combination of the incoherent (random) phase components of the pressure waves (see reference [5] for more details) and which can be described by the following equation (20.37) of Bass and Fuks [6]:

$$l(\mathbf{k}_1, \mathbf{k}_2) = \frac{\rho(\mathbf{q})\, l_{inc}\, S_0}{4} \frac{|\mathbf{q}|^4}{q_z^4}\, w(\boldsymbol{\gamma} = -\mathbf{q}_n),$$

$$\mathbf{q} = \mathbf{k}_2 - \mathbf{k}_1 \quad \mathbf{q}_n = \left(\frac{\mathbf{q}_x}{\mathbf{q}_z}, \frac{\mathbf{q}_y}{\mathbf{q}_z}\right). \tag{3}$$

This is the average scattered intensity (W/sr) for all random rough surfaces described by the same statistical distribution of slopes $w(\boldsymbol{\gamma})$, $\boldsymbol{\gamma}$ being the symbol for the slope $(\partial\xi/\partial x, \partial\xi/\partial y)$. I_{inc} is the intensity (W/m^2) of the incident plane wave, S_0 is the projection of the rough surface in the mean plane of the corrugations ($z = 0$) and $\rho(\mathbf{q})$ is the Fresnel reflection factor $|C_r|^2$ of the facets which reflect specularly from $\mathbf{k}_1$ to $\mathbf{k}_2$. The local normal vector of these facets is denoted by $\mathbf{q}$.

It can be shown that all the conditions under which equation (3) has been established are fulfilled in the limits of geometrical acoustics, provided that the detector R is far enough from the center of the rough surface and that the surface is sufficiently rough. It is clear that phase effects are not completely included in this model. Only the interferences in the specular direction are accounted for in the coherent term. Furthermore, the incoherent intensity will be viewed in section 3 as the result of several mirror facets reflecting in all directions. Therefore, the interference effects created between the waves emerging from the same facet are included in the model, but not those between facets. As long as geometrical acoustics is considered, these phase effects are of course limited.

In room acoustics, the coherent intensity is modelled by a specular ray or by a mirror image source, whereas the incoherent term, equation (3), gives rise to several techniques which are implemented independently or in parallel with the sound ray process. The coherent intensity is not discussed further in this paper. Equation (3) is now developed for a Gaussian rough surface, whose statistical distribution of slopes is

$$w(\boldsymbol{\gamma}) = \frac{T^2}{4\pi\sigma^2}\, \mathrm{e}^{-T^2|\gamma|^2/4\sigma^2} \tag{4}$$

where σ is the r.m.s. surface height and T is the correlation length (following the symbol conventions of Beckmann and Spizzichino [5]). The scattering direction $\mathbf{k}_2$ is referenced (as usual) by two scattering angles θ_2 and ϕ_2 (see Figure 1), which

yields

$$l(\theta_1, \theta_2, \phi_2) = \frac{\rho(\theta_s) l_{inc} S_0}{4} \left(\frac{T^2}{4\pi\sigma^2} \right) \frac{1}{\cos^4 \alpha} \, \mathrm{e}^{-T^2 \tan^2 \alpha / 4\sigma^2},$$

$$\cos 2\theta_s = \cos \theta_1 \cos \theta_2 - \sin \theta_1 \sin \theta_2 \cos \phi_2,$$

$$\frac{1}{\cos^4 \alpha} = \frac{|\mathbf{q}|^4}{q_z^4} = \frac{4(1 + \cos 2\theta_s)^2}{(\cos \theta_1 + \cos \theta_2)^4}. \tag{5}$$

In equation (5), the angle θ_s is the local angle of incidence on the specularly oriented facets and α is the angle between the normal to these facets and $\mathbf{1}_z$. This expression gives the KA angular distribution of the mean intensity scattered by a Gaussian rough surface.

KA theory neither takes into account the influence of the shadows cast by the elements of the rough surface on other elements nor considers the interception of some scattered waves by these elements. Both influences are often called "shadowing effects". For the limiting value ($\lambda \to 0$), Bass and Fuks [6] have shown that these effects can be modelled by the multiplication of equations (3) or (5) by a "shadowing function" $Q(\mathbf{k}_1, \mathbf{k}_2)$, which depends on the roughness parameters of the surface and, of course, on the directions of incidence and scattering. This additional factor Q can be interpreted as the proportion of specularly oriented facets that are actually viewed by the source (along $\mathbf{k}_1$) and the detector (along $\mathbf{k}_2$):

$$Q(\mathbf{k}_1, \mathbf{k}_2) = \frac{w_{ilv}(\boldsymbol{\gamma} = -\mathbf{q}_n; \mathbf{k}_1; \mathbf{k}_2)}{w(\boldsymbol{\gamma} = -\mathbf{q}_n)}. \tag{6}$$

The statistical distribution w_{ilv} is related to the slopes of those facets that are actually "illuminated" by the source and visible to the detector. Various analytical expressions will later be proposed for this shadowing function.

3. RAY ACOUSTICS

3.1. EQUIVALENCE WITH KA THEORY

It is shown in this section that the sound ray technique leads to the same expression as equation (3), which was derived from the KA theory, as developed for the limiting value ($\lambda \to 0$). As far as the author knows, this equivalence has not been explicitly proved elsewhere in the literature.

Consider again an incident plane wave propagating in the direction $\mathbf{k}_1$ to the rough surface S (Figure 1). The incident plane wave is now represented by a uniform bundle of N parallel sound rays, each ray carrying an equal part of the incident power:

$$W_r = \frac{l_{inc} S_0 \cos \theta_1}{N}. \tag{7}$$

Each sound ray is specularly reflected in a direction determined by the local slope at the point of intersection of the ray with the rough surface. The number of sound rays collected by the element of surface dS (with co-ordinates x, y and unit normal vector $\mathbf{n}$) is proportional to the area of this element projected in a plane perpendicular to the incident vector $\mathbf{k}_1$:

$$dN(x, y) = \left(\frac{N}{S_0 \cos\theta_1}\right) \frac{-\, dS\, \mathbf{k}_1 \cdot \mathbf{n}(x, y)}{k} = \left(\frac{N}{S_0 \cos\theta_1}\right) (\gamma_x \sin\theta_1 + \cos\theta_1)\, dx\, dy. \tag{8}$$

All these sound rays are reflected in the same direction $\mathbf{k}_2$, determined by the incident wave vector $\mathbf{k}_1$ and the local slope $\boldsymbol{\gamma}$. The total number of rays reflected in the solid angle $d\Omega$ around $\mathbf{k}_2$ ($d\Omega = \sin\theta_2\, d\theta_2\, d\phi_2$) is given by the integral of equation (8) over all visible parts of S_0 having the same slope ($\boldsymbol{\gamma} = -\mathbf{q}_n$):

$$dN(d\Omega) = N(1 - q_{nx} \tan\theta_1) \frac{1}{S_0} \int_{S_0} U(x, y \,|\, \boldsymbol{\gamma} \in \mathbf{D}(\boldsymbol{\gamma} = -\mathbf{q}_n))\, dx\, dy. \tag{9}$$

The function $U = 1$ if the slope of the rough surface at (x, y, ξ) is such that the sound rays are reflected in the solid angle $d\Omega$ *and* if this point is viewed by both the source (along $\mathbf{k}_1$) and the detector (along $\mathbf{k}_2$); otherwise $U = 0$. $D(\boldsymbol{\gamma} = -\mathbf{q}_n)$ is the domain of the variables (γ_x, γ_y) which is associated with the domain $d\Omega$ of the variables (θ_2, ϕ_2).

Therefore, the integral in equation (9) is the proportion of the horizontal surface S_o occupied by the specularly oriented elements dS that are viewed by both the source and the detector. If the rough surface is a random rough surface, this is precisely the product of the probability density function of the slopes $w_{ilv}(\boldsymbol{\gamma} = -\mathbf{q}_n; \mathbf{k}_1; \mathbf{k}_2)$ and the size of the domain $D(\boldsymbol{\gamma} = -\mathbf{q}_n)$. This size is calculated in Appendix A (equation (A4)).

Finally, recalling that the power carried by each scattered sound ray of this bundel is $\rho(\theta_s)W_r$, one obtains the total power scattered in the solid angle $d\Omega$ as

$$W_{\text{scat}}(d\Omega) = l_{inc}\, \rho(\theta_s) S_0 (\cos\theta_1 - q_{nx} \sin\theta_1)\, w_{ilv}(\boldsymbol{\gamma} = -\mathbf{q}_n; \mathbf{k}_1; \mathbf{k}_2)$$

$$\times \frac{d\Omega}{2\cos^2\alpha(\cos\theta_1 + \cos\theta_2)} \tag{10}$$

Therefore, if the definitions found in equation (5) are applied, the expression (3) for the scattered intensity (in W/sr) associated with the shadowing function in equation (6) is retrieved.

It must be noted that equation (8) introduces the limitation ($\mathbf{k}_1 \cdot \mathbf{n} < 0$), which expresses that the sound wave must reach the "positive" side of the surface element (i.e., the side facing the outer medium). This limitation does not explicitly appear in the last formulation (10), because the surface elements which do not fulfill it are not

directly "illuminated" by the sound source, and they are therefore automatically excluded from equation (10) by the function w_{ilv}.

3.2. STATISTICAL DISTRIBUTION OF THE SLOPES OF THE ROUGH SURFACE

The solution of equation (10) still requires the knowledge of the probability density function (p.d.f) w_{ilv}. However, only $w(\boldsymbol{\gamma})$ could possibly be derived from a statistical analysis of the profile of the rough surface. Moreover, this statistical analysis will often issue only some roughness parameters, and the p.d.f. $w(\boldsymbol{\gamma})$ will then be approximated, for example by a Gaussian law.

To derive w_{ilv} from $w(\boldsymbol{\gamma})$, the expression of the shadowing function must be known (see equation (6)). Several expressions are found in the literature [6, 8, 21]. The shadowing function discussed in this paper has been chosen because it allows extending the formalism to the second order reflections.

First, consider the case of backscattering ($\phi_2 = \pi$), when the incident vector ($\mathbf{k}_1$) is closer to grazing than the scattered vector ($\mathbf{k}_2$). In this case, the conditional probability that a sound ray reflected along $\mathbf{k}_2$ directly escapes from the rough surface if $\mathbf{k}_1$ has not been stopped is equal to one. Therefore, the p.d.f. w_{ilv} does not depend on $\mathbf{k}_2$, but only on $\mathbf{k}_1$.

It is assumed that $w_{ilv}(\boldsymbol{\gamma}; \mathbf{k}_1)$ is proportional to $w(\boldsymbol{\gamma})$, for $(\gamma_x \sin\theta_1 + \cos\theta_1 \geqslant 0)$. For other values of γ_x, w_{ilv} vanishes, since the corresponding surface elements are not directly illuminated. This assumption is corroborated by the works of Bass and Fuks [6] (see their equation (23.28)):

$$w_{ilv}(\boldsymbol{\gamma}; \mathbf{k}_1) = \alpha_w w(\boldsymbol{\gamma}) \Theta(\gamma_x \sin\theta_1 + \cos\theta_1),$$

$$\alpha_w \int_{-\cot\theta_1}^{+\infty} \mathrm{d}\gamma_x \int_{-\infty}^{+\infty} (\gamma_x \tan\theta_1 + 1) w(\boldsymbol{\gamma})\, \mathrm{d}\gamma_y = 1. \tag{11}$$

In this equation, $\Theta(x) = 1$ for $x \geqslant 0$ and $\Theta(x) = 0$ for $x < 0$. The constant α_w is determined in equation (11) by the condition that the total number of rays N must be equal to the integral of the number of rays received by all elements of the rough surface. This number is derived from equation (9) and will be expressed later in equation (15). For a Gaussian rough surface, the following expression for the constant α_w can be found in reference [6]:

$$\alpha_w = \frac{1}{1 + \Lambda_N((T/\sigma\sqrt{2})\cot\theta_1)}, \quad \Lambda_N(a) = \frac{1}{2a}\left(\sqrt{\frac{2}{\pi}}\, \mathrm{e}^{-a^2/2} - a\, \mathrm{erfc}\left(\frac{a}{\sqrt{2}}\right)\right). \tag{12}$$

The product $\alpha_w \Theta(\gamma_x \sin\theta_1 + \cos\theta_1)$ in equation (11) is interpreted as the conditional probability that the elements of the rough surface are viewed by the incident wave, if they have the slope $\boldsymbol{\gamma}$. Therefore, if the scattered vector $\mathbf{k}_2$ is now closer to grazing than $\mathbf{k}_1$, it determines the same expression for the conditional probability, with the angle θ_2 replacing θ_1 in equations (11) and (12).

In the case of forward scattering ($\phi_2 = 0$), it can be assumed that both conditional probabilities (along $\mathbf{k}_1$ and $\mathbf{k}_2$) are independent, which, for a Gaussian rough surface, leads to

$$w_{ilv}(\boldsymbol{\gamma}; \mathbf{k}_1; \mathbf{k}_2) = \beta_w w(\boldsymbol{\gamma}) \Theta(\gamma_x + \cot\theta_1) \Theta(\cot\theta_2 - \gamma_x),$$

$$\beta_w = \frac{1}{(1 + \Lambda_N((T/\sigma\sqrt{2})\cot\theta_1))(1 + \Lambda_N((T/\sigma\sqrt{2})\cot\theta_2))}. \tag{13}$$

However, the independence of the conditional probabilities is only valid, strictly speaking, for a single facet. If all sound rays reaching the rough surface along $\mathbf{k}_1$ are considered, then their associated obstruction or visibility can influence the probability of being reflected along $\mathbf{k}_2$. Bass and Fuks [6] propose another expression to take this dependence into account (their equation (23.38.c). This expression introduces some significant differences, mainly at grazing incidence and scattering angles.

Finally, if the scattering direction $\mathbf{k}_2$ is not in the plane of incidence, then the shadowing function explicitly depends on the azimuth ϕ_2. In that case, no simple relation has been found in the literature, and the following general formulation is adopted:

$$w_{ilv}(\boldsymbol{\gamma}; \mathbf{k}_1; \mathbf{k}_2) = S(\theta_1, \theta_2, \phi_2) w(\boldsymbol{\gamma}) \Theta(\gamma_x + \cot\theta_1) \Theta(\cot\theta_2 - \gamma_\phi),$$

$$\gamma_\phi = \gamma_x \cos\phi_2 + \gamma_y \sin\phi_2. \tag{14}$$

3.3. A SOUND RAY ALGORITHM TO MODEL THE KA SCATTERING PROCESS

This algorithm can be applied to any sound ray technique which is based on a random sampling of rays emitted from the source. Any sound ray reaching a diffusing rough surface is reflected in a random direction. This algorithm will determine the random direction in such a way that, considering the whole process, the distribution of the scattered intensity (10) predicted by the KA theory is retrieved.

The algorithm is based on the following: each sound ray reaching the rough surface belongs to a bundle of N parallel rays, modelling a plane wave. Strictly speaking, this can be assumed if the distance covered by the ray from the source (or from the last reflection) is long enough. The probability for this ray to fall on a facet having the slope $\boldsymbol{\gamma}$ is similar to equation (9):

$$\frac{\mathrm{d}N(\boldsymbol{\gamma})}{N} = (\gamma_x \tan\theta_1 + 1) w_{ilv}(\boldsymbol{\gamma}; \mathbf{k}_1)\, \mathrm{d}\gamma_x\, \mathrm{d}\gamma_y. \tag{15}$$

Only the obstructions of the incident rays along $\mathbf{k}_1$ are presently considered. The obstructions of the scattered rays will be considered further. The following

cumulative distributions will be used in the algorithm:

$$F(\gamma_x) = \frac{1}{N} \int_{-\cot\theta_1}^{\gamma_x} \int_{-\infty}^{+\infty} \mathrm{d}N(\boldsymbol{\gamma}'), \qquad F(\gamma_y) = \frac{1}{N} \int_{-\cot\theta_1}^{+\infty} \int_{-\infty}^{\gamma_y} \mathrm{d}N(\boldsymbol{\gamma}'). \tag{16}$$

The algorithm is now described step by step: any sound ray incident on the rough surface along $\mathbf{k}_1$ defines on that surface a local axis system $\mathbf{1}_x$ and $\mathbf{1}_y$ (Figure 1). It is assumed that the statistical distribution of the slopes is known in this system.

Step 1: Generate two random numbers X and Y between 0 and 1 (uniform p.d.f.) and solve the equations $X = F(\gamma_x)$ and $Y = F(\gamma_y)$, which give the slopes γ_x and γ_y.

Step 2: Calculate the normal vector $\mathbf{n}$ corresponding to these slopes, and the new direction of the ray given by $\mathbf{k}_2 = \mathbf{k}_1 - 2(\mathbf{k}_1 \cdot \mathbf{n})\mathbf{n}$.

Step 3: Account for the probability of obstruction of $\mathbf{k}_2$, by generating a third random number Z between 0 and 1 (uniform p.d.f.): If $(\alpha_w Z) \leqslant S(\theta_1, \theta_2, \phi_2)$, then the sound ray escapes from the rough surface and its power is multiplied by $\rho(\theta_s)$; otherwise, it is obstructed. This last step of course requires the knowledge of $S(\theta_1, \theta_2, \phi_2)$.

This algorithm has been applied to the particular case of a perfectly hard ($\rho = 1$) Gaussian rough surface, for which equation (16) can be written as

$$F(\gamma_x) = \frac{\Lambda_N(a) - \Lambda_N(a; b)}{1 + \Lambda_N(a)} \quad (\text{for } b \geqslant -a), \quad F(\gamma_y) = 1 - 0{\cdot}5 \operatorname{erfc}\left(\frac{T\gamma_y}{2\sigma}\right)$$

$$\Lambda_N(a; b) = \frac{1}{2a}\left(\sqrt{\frac{2}{\pi}}\, \mathrm{e}^{-b^2/2} - a \operatorname{erfc}\left(\frac{-b}{\sqrt{2}}\right)\right), \quad a = \frac{T}{\sigma\sqrt{2}} \cot\theta_1, \quad b = \frac{T\gamma_x}{\sqrt{2}\sigma}. \tag{17}$$

Figures 3 and 4 show the results of several applications of this algorithm. The scattered rays are collected in small finite solid angles which are defined by $\Delta\phi_2 = 10^\circ$ and $\Delta\theta_2 = 5^\circ$. The collected power is then compared with the theoretical expression of equation (10), in the plane of incidence. Step 3 of the algorithm has not been applied here, since a more precise definition of $S(\theta_1, \theta_2, \phi_2)$ must still be found.

These results clearly show that the proposed algorithm generates scattered intensities which approach the ones predicted by KA theory, as the total number of rays N grows. An important conclusion from this application is that the scattering process cannot be simply modelled independently of the angle of incidence: Indeed, equation (17) clearly shows that the random generation of slopes (γ_x, γ_y) is influenced by θ_1. This prevents the formulation of an algorithm in which the slopes would be generated at once for each rough surface, at the beginning of the process. Therefore, the slopes must be generated during the sound rays' process, for two

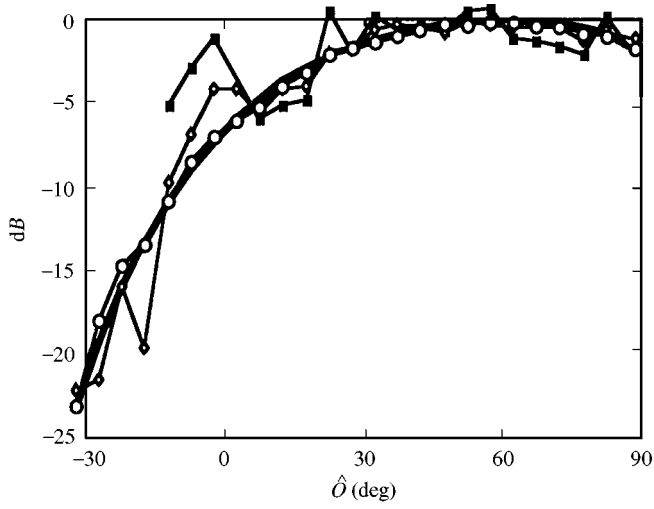

Figure 3. Distributions of the scattered intensity in the plane of incidence obtained by KA theory (equation (10)) and by three executions of the algorithm defined in Section 3.3: $N = 10^3$, 10^4 and 10^5 rays. The angle of incidence is $\theta_1 = 60^\circ$ and the perfectly hard rough surface has a Gaussian distribution of slopes with r.m.s. slope = 0.28 ($T/\sigma = 5$). The scattered power per unit solid angle has been normalized to 0 dB in the specular direction (observation angle $\hat{O} = \theta_2 = +60^\circ$). Negative observation angles correspond to backward scattering ($\hat{O} = -\theta_2$). —, KA; –■–, 1000; –◇–, 10 000; –○–, 100 000.

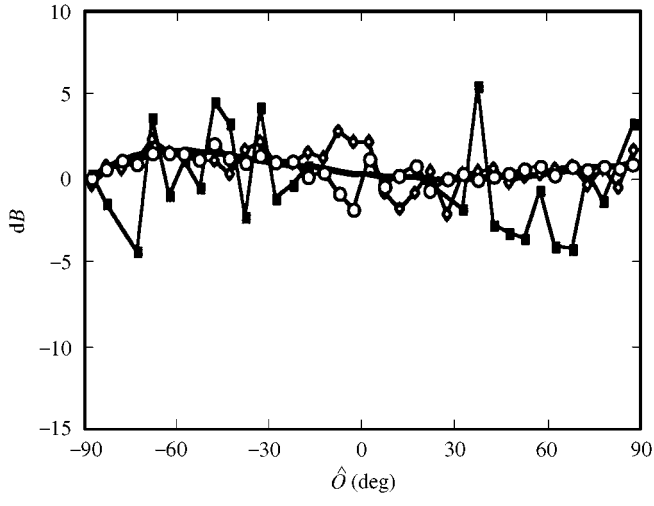

Figure 4. Same as Figure 3 with 30° angle of incidence and a r.m.s. slope = 0.71 ($T/\sigma = 2$). The scattered power per unit solid angle has still been normalized to 0 dB in the specular direction ($\hat{O} = \theta_2 = +30^\circ$). —, KA; –■–, 1000; –◇–, 10 000; –○–, 100 000.

reasons:

—first, some slopes must be eliminated for a given angle of incidence ($\gamma_x \sin\theta_1 + \cos\theta_1 \geqslant 0$);
—second, the initial distribution $w(\boldsymbol{\gamma})$ must be corrected by $(\gamma_x \tan\theta_1 + 1)$: see equation (15).

Finally, it must be noted that the algorithm described in this paper is not limited to random rough surfaces. Indeed, the only reference to a random process has been the replacement of the integral in equation (9) by the p.d.f. of the slopes. If the surface is instead described by an analytical function $z = \xi(x, y)$ such that the z-component of the normal vector is always positive, then the developments are still valid, provided that the integral in equation (9) can be calculated.

4. SECOND-ORDER REFLECTIONS

4.1. MODELLING

The analysis of the sound ray process is now extended to second-order reflections. It has already been mentioned that the classical formulation of the KA theory does not take these effects of multiple scattering into account. Several authors [9, 12, 22, 23] have proposed extensions of the KA to model multiple scattering, but their formulations generally imply the generation of sample profiles of rough surfaces. In this paper, it is attempted instead of derive general developments which avoid the generation of particular rough surfaces. This will in turn require the formulation of a hypothesis in order to find a general expression for the second order scattering.

Consider again the number of sound rays reflected by the rough surface, which results in the expression of equation (10). The proportion $S(\theta_1, \theta_2, \phi_2)/\alpha_w(\theta_1)$ effectively escapes from the rough surface in the scattering direction (θ_2, ϕ_2), and the complementary proportion $(1 - (S/\alpha_w))$ corresponds to the rays which fall on other facets of the surface and are again reflected. The number of sound rays reflected in the solid angle $\mathrm{d}\Omega_2$ around the direction (θ_2, ϕ_2) which undergoes a second reflection on the rough surface is derived from equations (9) and (10):

$$\mathrm{d}N(\mathrm{d}\Omega_2) = N(1 - q_{nx}\tan\theta_1)(\alpha_w - S)\,w(\boldsymbol{\gamma} = -\mathbf{q}_n)\,\frac{\Theta(-\mathbf{q}_{nx} + \cot\theta_1)\,\mathrm{d}\Omega_2}{2\cos^2\alpha(\cos\theta_1 + \cos\theta_2)}. \quad (18)$$

It is again assumed that the probability for a ray in this bundle to fall on a facet with slope $\boldsymbol{\gamma}$ is proportional to the projected area of this facet and to the p.d.f. of the slopes:

$$\frac{\mathrm{d}^2 N(\boldsymbol{\gamma}')}{\mathrm{d}N(\mathrm{d}\Omega_2)} = \eta(\theta_2, \phi_2)\,(\sin\theta_2\,\gamma'_\phi - \cos\theta_2)\,w(\boldsymbol{\gamma}')\,\Theta(\gamma'_\phi - \cot\theta_2)\,\mathrm{d}\gamma'_x\,\mathrm{d}\gamma'_y, \quad (19)$$

where γ'_ϕ is defined as γ_ϕ in equation (14). This simple assumption is, until now, only supported by its validity for the entire incident bundle on the rough surface. A more detailed analysis is still required to verify this assumption for particular rough surfaces. However, it can be investigated whether any useful analytical expression can be derived from equation (19).

The constant of proportionality $\eta(\theta_2, \phi_2)$ is evaluated by expressing that the integral of $d^2N(\boldsymbol{\gamma}')$ for all possible values of $\boldsymbol{\gamma}'$ gives $dN(d\Omega_2)$:

$$(\eta(\theta_2, \phi_2))^{-1} = \int_{\cot\theta_2}^{+\infty} du \int_{-\infty}^{+\infty} (u \sin\theta_2 - \cos\theta_2) w(u, v)\, dv$$

$$w(u, v) = w(\boldsymbol{\gamma}'(u, v)), \qquad \gamma'_x = u\cos\phi_2 - v\sin\phi_2 \quad \text{and} \quad \gamma'_y = u\sin\phi_2 + v\cos\phi_2. \tag{20}$$

The sound rays falling on a facet with slope $\boldsymbol{\gamma}'$ are reflected in a direction $\mathbf{k}_3$, defined by the angles (θ_3, ϕ_3):

$$\mathbf{p} = \mathbf{k}_3 - \mathbf{k}_2, \quad \gamma'_x = -\frac{p_x}{p_z} = -p_{nx}, \qquad \gamma'_y = -\frac{p_y}{p_z} = -p_{ny}. \tag{21}$$

The number of rays reflected in a solid angle $d\Omega_3$ surrounding the direction $\mathbf{k}_3$ can be evaluated as in equation (10), i.e., deriving it from $d^2N(\boldsymbol{\gamma}')$. Integrating for all possible values of (θ_2, ϕ_2) will then give the total number of rays reflected in $d\Omega_3$:

$$dN(d\Omega_3) = N \frac{\alpha_w(\theta_1)\, d\Omega_3}{16\cos\theta_1} \int_0^{2\pi} d\phi_2 \int_{\theta_3}^{\pi-\theta_1} H_{13}(\theta_2, \phi_2) \sin\theta_2\, d\theta_2,$$

$$H_{13}(\theta_2, \phi_2) = \left(1 - \frac{S(\theta_1, \theta_2, \phi_2)}{\alpha_w(\theta_1)}\right) \frac{w(\boldsymbol{\gamma} = -\mathbf{q}_n)}{\cos^4\alpha}\, \eta(\theta_2, \phi_2)\, \frac{w(\boldsymbol{\gamma} = -\mathbf{p}_n)}{\cos^4\beta},$$

$$\frac{1}{\cos^2\beta} = \frac{|\mathbf{p}|^2}{p_z^2}. \tag{22}$$

Some of these rays are again blocked by the rough surface itself. As discussed previously, this can be taken into account by the introduction of a shadowing function in equation (22). This function depends on the roughness profile of the surface, and on the successive paths followed by the sound rays before they escape from the surface; it is called $T(\mathbf{k}_1, \mathbf{k}_2, \mathbf{k}_3)$ and will not be analyzed further in this paper. It is only mentioned that this function must be such that the principle of reciprocity is fulfilled. This principle is recalled as follows: If a sound wave impinging on a surface along the incident vector $\mathbf{k}_1$ produces a scattered power (per unit solid angle) in the direction $\mathbf{k}_3$, then the same effect is obtained if the sound wave is incident along $(-\mathbf{k}_3)$ and the detector placed along $(-\mathbf{k}_1)$. The power scattered per unit solid angle is given by the equation

$$l_r(\mathbf{k}_3) = \frac{l_{inc} S_0}{16}\, \alpha_w(\theta_1) \int_0^{2\pi} d\phi_2 \int_{\theta_3}^{\pi-\theta_1} H_{13}(\theta_2, \phi_2) \rho(\theta_s) \rho(\theta'_s)\, T(\mathbf{k}_1, \mathbf{k}_2, \mathbf{k}_3) \sin\theta_2\, d\theta_2. \tag{23}$$

Interchanging the direction of incidence $\mathbf{k}_1$ and the direction of scattering $\mathbf{k}_3$ leads to the following expression of the principle of reciprocity:

$$(\alpha_w(\theta_1) - S(\theta_1, \theta_2, \phi_2))\eta(\theta_2)\, T(\mathbf{k}_1, \mathbf{k}_2, \mathbf{k}_3) = (\alpha_w(\theta_3) - S(\theta_3, \pi - \theta_2, \phi_2 - \phi_3))$$

$$\times \eta(\pi - \theta_2)\, T(-\mathbf{k}_3, -\mathbf{k}_2, -\mathbf{k}_1). \tag{24}$$

This condition is formulated for a particular class of rough surfaces called isotropic surfaces, for which there is no azimuthal dependence in the statistical distribution of the slopes. Therefore, the expression of $\eta(\theta_2, \phi_2)$ in equation (20) can be reduced to $\eta(\theta_2)$.

Equation (23) could be used as an expression for analyzing second-order scattering effects. However, it will be shown hereafter that it leads to strange results in some particular situations. This in turn will cast some doubt on the simple assumption in equation (19). Consider the case illustrated in Figure 5, which leads to

—$S(\theta_1, \theta_2, \phi_2 = \pi) = \alpha_w(\theta_2)$;
—$T(-\mathbf{k}_3, -\mathbf{k}_2, -\mathbf{k}_1) = 1$, since all sound rays reflected along $-\mathbf{k}_1$ will leave the surface if $-\mathbf{k}_3$ and $-\mathbf{k}_2$ are not blocked;
—$S(\theta_3, \pi - \theta_2, \phi_2 - \phi_3) = 0$, since $\pi - \theta_2 > \pi/2$.

Applying the principle of reciprocity as in equation (24) gives (see also Appendix B)

$$T(\mathbf{k}_1, \mathbf{k}_2, \mathbf{k}_3) = \frac{\alpha_w(\theta_3)}{\alpha_w(\theta_1) - \alpha_w(\theta_2)} \frac{\eta(\pi - \theta_2)}{\eta(\theta_2)} = \frac{\alpha_w(\theta_3)(1 - \alpha_w(\theta_2))}{\alpha_w(\theta_1) - \alpha_w(\theta_2)}. \tag{25}$$

This expression for the shadowing function leads to infinite values if the angle θ_2 approaches θ_1. This is not consistent with the definition of such a function, which should be limited between 0 and 1.

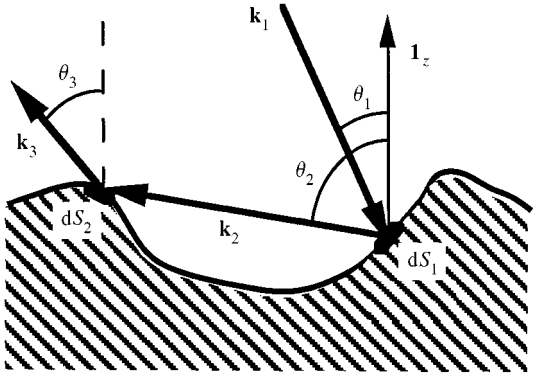

Figure 5. Scattering geometry illustrating the limitation of the simple hypothesis in equation (19). First reflection occurs at dS_1 and second reflection at dS_2. In this case, $\phi_2 = \phi_3 = \pi$ and $\theta_1 < \theta_3 < \theta_2 < \pi/2$.

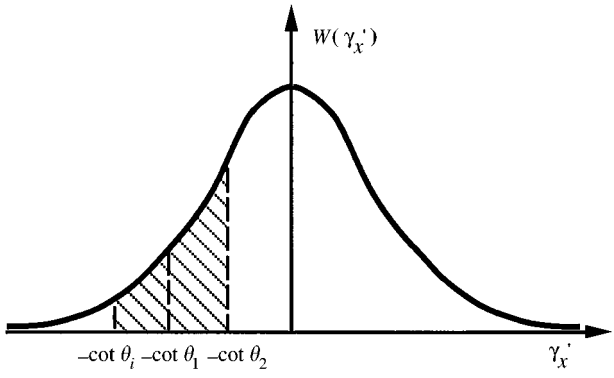

Figure 6. Statistical distribution of the slopes γ_x' for a random rough surface. The hatched region illustrates the interval containing the slopes' permitted values, in the backscattering case ($\phi_2 = \pi$) and $\theta_1 < \theta_2 < \pi/2$. The angle θ_i is defined in the text.

An explanation for this problem can be found if the assumption in equation (19) is again considered. The condition stating that the sound ray along $\mathbf{k}_2$ hits the positive side of the rough surface is expressed by $\Theta(\gamma_\phi' - \cot\theta_2) = 1$, or $\gamma_x' < -\cot\theta_2$ in the situation illustrated in Figure 5. This is a first limitation on the slope of the surface at $\mathrm{d}S_2$. However, there is another condition which has not been taken into account in equation (19). It states that the slope cannot be too steep at $\mathrm{d}S_2$, as θ_2 approaches θ_1; otherwise, the ray $\mathbf{k}_1$ would be blocked. In the limiting case ($\theta_2 = \theta_1$, $\phi_2 = \pi$), the only possible value becomes $\gamma_x' = -\cot\theta_2 = -\cot\theta_1$. This condition on the slope of the surface at $\mathrm{d}S_2$ seems responsible for the inconsistency found above in equation (25). Therefore, it is proposed to modify equation (19) as follows:

$$\frac{\mathrm{d}^2 N(\boldsymbol{\gamma}')}{\mathrm{d}N(\mathrm{d}\Omega_2)} = F(\theta_1, \theta_2, \phi_2)\,\eta(\theta_2, \phi_2)((\sin\theta_2\,\gamma_\phi' - \cos\theta_2)\,w(\boldsymbol{\gamma}')\,\Theta(\gamma_\phi' - \cot\theta_2)$$

$$\times\,\Theta(\cot\theta_i - \gamma_\phi')\,\mathrm{d}\gamma_x'\,\mathrm{d}\gamma_y',$$

$$F(\theta_1, \theta_2, \phi_2) = \left(1 - \frac{\eta(\theta_2, \phi_2)}{\eta_{ext}(\theta_i, \theta_2, \phi_2)}\right)^{-1},$$

$$(\eta_{ext}(\theta_i, \theta_2, \phi_2))^{-1} = \int_{\cot\theta_i}^{+\infty} \mathrm{d}u \int_{-\infty}^{+\infty} (u\sin\theta_2 - \cos\theta_2)\,w(u, v)\,\mathrm{d}v. \tag{26}$$

As discussed previously, the constant of proportionality is evaluated by expressing that the integral of $\mathrm{d}^2 N(\boldsymbol{\gamma}')$, for all possible values of $\boldsymbol{\gamma}'$, gives $\mathrm{d}N(\mathrm{d}\Omega_2)$. The angle θ_i has been introduced to limit the slope of the surface at $\mathrm{d}S_2$. This is illustrated in the

case of backscattering by Figure 6: as θ_2 approaches θ_1, the angle θ_i moves from 0 to θ_1.

The value of θ_i is not prescribed here, leaving some freedom to the model. The conditions that must be fulfilled by this angle are the following:

—$0 \leqslant \theta_i \leqslant \theta_1 < \theta_2 \leqslant \pi/2$. If $\theta_2 \leqslant \theta_1$, then $\theta_i = \theta_2$, which leads to $\mathrm{d}^2 N(\boldsymbol{\gamma}') = 0$ in equation (26);
—if $\theta_2 > \pi/2$, then $\theta_i = 0$, which expresses that the ray $\mathbf{k}_1$ has no influence in this case;
—θ_i is a monotonically increasing function of $\theta_1 < \theta_2$, for a fixed value of θ_2.

The condition $\theta_i < \theta_2$ implies that $F \geqslant 1$, in equation (26). This function and the angle θ_i are closely related to each other. Defining F will automatically define θ_i according to equation (26).

With this new assumption, the power reflected per unit solid angle is now given by

$$l_r(\mathbf{k}_3) = \frac{l_{inc} S_0}{16} \alpha_w(\theta_1) \int_0^{2\pi} \mathrm{d}\phi_2 \int_{\theta_3}^{\pi-\theta_1} \mathbf{J}(\theta_1, \theta_2, \phi_2) \rho(\theta_s) \rho(\theta_s') T(\mathbf{k}_1, \mathbf{k}_2, \mathbf{k}_3)$$

$$\times \Theta(\cot\theta_i - \gamma_\phi') \sin\theta_2 \, \mathrm{d}\theta_2,$$

$$J(\theta_1, \theta_2, \phi_2) = H_{13}(\theta_2, \phi_2) F(\theta_1, \theta_2, \phi_2). \tag{27}$$

In equation (27), γ_ϕ' is evaluated for $(\boldsymbol{\gamma}' = -\bar{p}_n)$ and the condition $\Theta(\cot\theta_i - \gamma_\phi') \neq 0$ can be usefully replaced by a reduction of the domain of integration:

$$\cos(\theta_2 - \theta_i) - \cos\theta_3 \cos\theta_i - \sin\theta_3 \sin\theta_i \cos(\phi_2 - \phi_3) \leqslant 0. \tag{28}$$

Applying the model of equation (27) would require the knowledge of $S(\theta_1, \theta_2, \phi_2)$, $F(\theta_1, \theta_2, \phi_2)$ and $T(\mathbf{k}_1, \mathbf{k}_2, \mathbf{k}_3)$. $S(\theta_1, \theta_2, \phi_2)$ is the shadowing function extended to the azimuthal dependence. $F(\theta_1, \theta_2, \phi_2)$ can be freely chosen in the model. However, it must be recalled that this function defines the angle θ_i, and that some conditions must be fulfilled by this angle. The definition of these three functions could also be guided by the statistical analysis of some particular slope distributions and the application of the principle of reciprocity. This work is still in progress. It will not be described here, as it would itself require an entire study.

4.2. FIRST RESULTS AND DISCUSSION

The first results of the modelling of second order scattering via equation (27) have been computed for isotropic surfaces, with the following functions:

$$F(\theta_1, \theta_2, \phi_2) = \frac{\alpha_w(\theta_1)(1 - \alpha_w(\theta_2))}{\alpha_w(\theta_1) - S(\theta_1, \theta_2, \phi_2)},$$

$$T(\mathbf{k}_1, \mathbf{k}_2, \mathbf{k}_3) = \frac{S(\theta_1, \theta_3, \phi_3)}{\alpha_w(\theta_1)} \quad \text{for } \theta_3 \leqslant \theta_2 \leqslant \pi - \theta_1,$$

$$T(\mathbf{k}_1, \mathbf{k}_2, \mathbf{k}_3) = 0 \quad \text{if } \cos(\pi - \theta_2 - \theta_i') - \cos\theta_1 \cos\theta_i' - \sin\theta_1 \sin\theta_i' \cos\phi_2 \geqslant 0. \tag{29}$$

F has been chosen to solve the problem of reciprocity found in equation (25). It can be shown that this function also fulfills the conditions imposed on the limiting angle θ_i, for isotropic surfaces. T is derived from the definition of F, through the principle of reciprocity. This is not a unique solution, but this expression gives a consistent simulation of shadowing after two reflections. In this definition, the angle θ_i' is derived from the definition of $F(\theta_3, \pi - \theta_2, \phi_2 - \phi_3)$, in the same manner as θ_i is derived from $F(\theta_1, \theta_2, \phi_2)$ in equation (26). Finally, the shadowing function $S(\theta_1, \theta_2, \phi_2)$ does not appear explicitly in equation (27), if the scattering is only evaluated in the plane of incidence where $S = \beta_w$ or $S = \alpha_w$. $S(\theta_1, \theta_2, \phi_2)$ is only needed in the determination of the angles θ_i and θ_i', which is not a critical step of the computation. Therefore, these first results have been computed with an approximation, i.e., a continuous variation of the shadowing function between the half-planes $\phi_2 = 0$ and $\phi_2 = \pi$:

$$S(\theta_1, \theta_2, \phi_2) = \alpha_w(\theta_1)\alpha_w(\theta_2)K(\phi_2) + (1 - K(\phi_2)) \min\{\alpha_w(\theta_1), \alpha_w(\theta_2)\},$$

$$K(\phi_2) = \left|\cos^3\frac{\phi_2}{2}\right|. \tag{30}$$

The formulation of $K(\phi_2)$ has been based on studies carried out for Gaussian rough surfaces.

Figure 7 shows some results calculated with equation (27), for a perfectly hard Gaussian rough surface. As could be expected, second order reflections are not significant for $T/\sigma = 10$, compared with the contribution of the first order reflections. Also for the slightly rough surface ($T/\sigma = 10$), the model predicts a nearly specular peak for the first order scattered intensity and an off-specular peak for the second order scattering. The nearly specular peak of the first order contribution is consistent with the maximum value of equation (5) in $\alpha = 0$. The shadowing function (which does not appear in equation (5)) does not have any significant influence on the location of this maximum in this case. However, it would be interesting to corroborate the existence of the second-order off-specular peak with other techniques. For the very rough surface ($T/\sigma = 1$), it is seen that neither the first nor the second order reflections create specular peaks, instead two maximum intensities, one in the backscattering half-plane and the other in the forward scattering half-plane.

Enhanced backscattering is created at greater r.m.s. slopes by both first and second order reflections. In the case of perfectly hard surfaces, the contribution of second order scattering becomes as important as (and sometimes even more than) first order scattering. For real surfaces (with $\rho < 1$), this importance would of course be reduced but could still be significant.

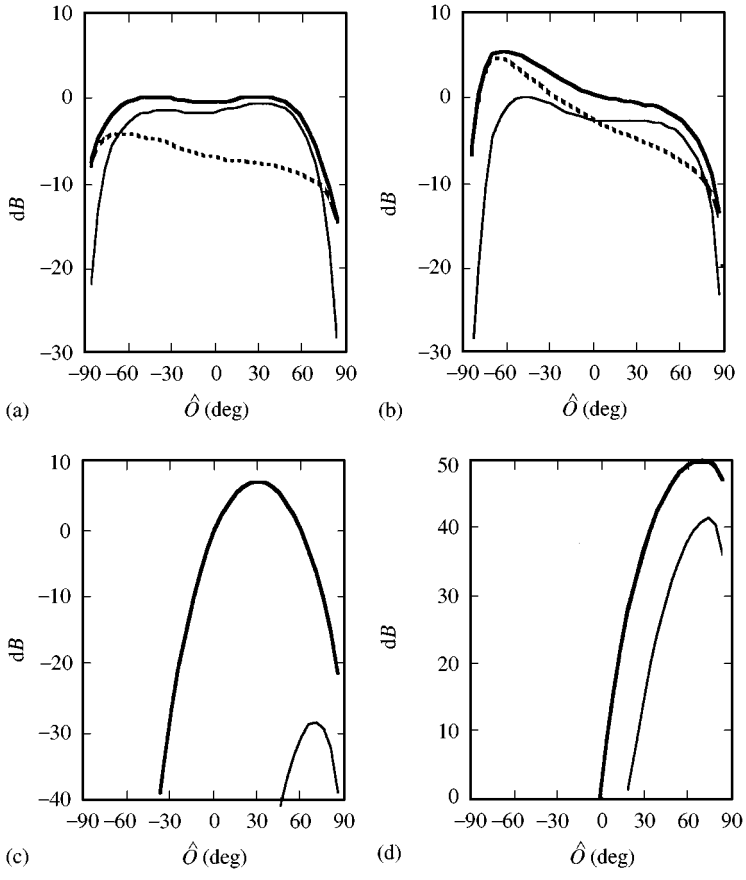

Figure 7. Distributions of the scattered intensity in the plane of incidence computed with equation (5) for the contribution of the first reflections (1 refl.) and with equation (27) for the contribution of the second reflections (2 refl.). The rough surface is Gaussian and perfectly hard. The total (Sum) scattered power per unit solid angle has been normalized to 0 dB in the direction of observation $\hat{O} = \theta_2 = 0°$. Negative observation angles correspond to backward scattering ($\hat{O} = -\theta_2$): (a) $\theta_1 = 30°$, r.m.s. slope = 1·4 ($T/\sigma = 1$); (b) $\theta_1 = 70°$, r.m.s. slope = 1·4; (c) $\theta_1 = 30°$, r.m.s. slope = 0·14 ($T/\sigma = 10$); (d) $\theta_1 = 70°$, r.m.s. slope = 0·14. In (c) and (d), the "1 refl." and "Sum" results are superimposed. - -, 1 refl.; —, 2 refl.; ——, Sum.

After these first calculations, it was attempted to test the validity of equation (27), associated with equations (29) and (30). In particular, a comparison with results (either measured or computed) published by other authors would be interesting. A survey of the literature has led to some results for 3D rough surfaces [10, 23, 24]. However, all of these are computed for slightly rough surfaces ($\sigma \sim \lambda$) and cannot be compared with geometrical acoustics solutions. For 2-D random surfaces, Macaskill [12] has published some distributions of scattered intensities computed with a ray algorithm. This algorithm has been applied to 40 realizations of 2-D Gaussian rough surfaces with r.m.s. slope 0·86. Moreover, Macaskill has presented the contributions of each order of reflection (up to the third) and this will allow an interesting comparison with the results based on equation (27).

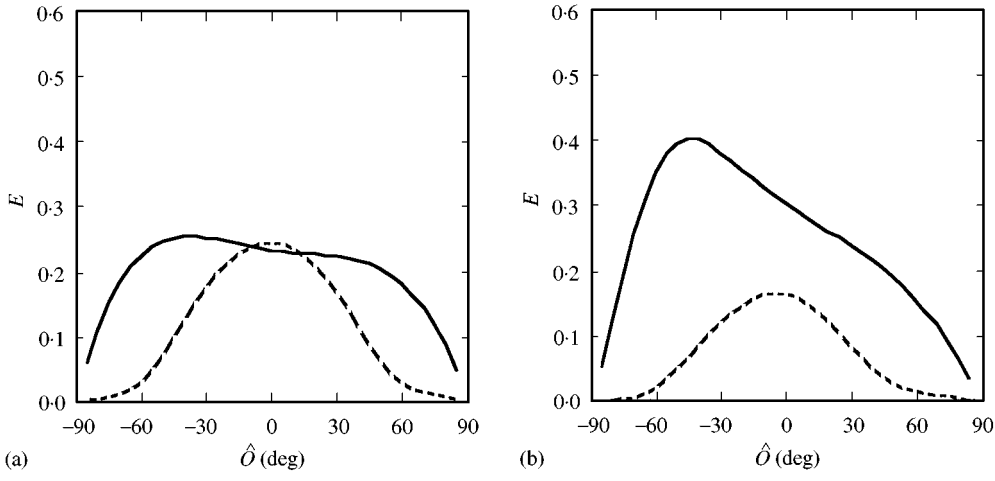

Figure 8. Distributions of the scattered intensity in the plane of incidence computed with equation (10) for the contribution of the first reflections (1 refl.) and with equation (27) for the contribution of the second reflections (2 refl.). The 2-D cylindrical rough surface is Guassian and perfectly hard, with $T/\sigma = 1{\cdot}64$. The scattered power per unit solid angle (E) has been normalized as in Macaskill's paper [12], so that the incident energy is unity: (a) $\theta_1 = 10^\circ$; (b) $\theta_1 = 40^\circ$. ——1 refl.; – – –, 2 refl.

Equation (27) has first been derived for 2-D cylindrical rough surfaces. Then, the distributions of scattered intensities have been computed in the plane of incidence, perpendicular to the cylindrical corrugations of the rough surface, for the angles of incidence 10 and 40°. Figure 8 shows the results, which can be directly compared with Figure 8 of Macaskill's paper [12].

The correspondence between first order scattering results is fairly good. For second order scattering effects, some differences are observed: the peak of intensity is stronger in Macaskill's results. It also occurs at greater forward scattering angles. But, the overall estimate is quite satisfying, for example concerning the relative importance between first and second order contributions, and between $\theta_1 = 10$ and 40°. Investigations are now being carried out to confirm these encouraging initial results and to extend the validity of the model.

5. CONCLUSIONS

In this paper, it is shown that the scattered power obtained by the first-order reflections of sound rays on a random rough surface is identical to that obtained by the KA theory developed in the geometrical acoustics limit ($\lambda \to 0$). This has been proved for any random surface and can be extended to deterministic surfaces, provided that the integral (9) can be calculated for their profile $z = \xi(x, y)$.

From this theoretical analysis, a sound ray algorithm has been derived to simulate KA scattering. This simple algorithm can be inserted into a more general room acoustics software based on the sound ray concept, in order to model sound scattering (as a substitute for Lambert's law, for example).

Finally, the sound ray process is extended to analyze second-order scattering effects. The point of interest here is that this model does not require the generation

of several rough surfaces profiles in order to derive significant results. However, the assumptions which have been formulated must still be corroborated by further works, for example by statistical analysis of real profiles. In particular, equation (26) and the mathematical functions expressed by equations (29) and (30) are still under study for better correspondence with the results of other approaches.

ACKNOWLEDGMENTS

The author would like to thank R. R. Torres of the Chalmers Room Acoustics Group in Göteborg for helpful discussion about this paper. The work is funded by the Belgian National Fund for Scientific Research.

REFERENCES

1. H. Kuttruff 1991 *Room Acoustics*, 282. Barking, England: Elsevier, third edition.
2. H. Kuttruff 1991 *Acustica* **75**, 99–104. Transiente Schallausbreitung in Flachräumen mit diffus reflektierenden Wänden.
3. M. R. Hodgson 1991 *Journal of the Acoustical Society of America* **89**, 765–771. Evidence of diffuse surface reflections in rooms.
4. Y. W. Lam 1996 *Journal of the Acoustical Society of America* **100**, 2181–2192. A comparison of three diffuse reflection modelling methods used in room acoustics computer models.
5. P. Beckmann and A. Spizzichino 1963 *The Scattering of Electromagnetic Waves from Rough Surfaces*. New York: Macmillan.
6. F. G. Bass and I. M. Fuks 1979 *Wave Scattering from Statistically Rough Surfaces*, Chapter 7. Oxford: Pergamon.
7. A. Ishimaru 1978 *Wave Propagation and Scattering in Random Media*, Vol. II, Chapter 21. New York: Academic Press.
8. J. J. Embrechts 1992 *Lighting Research and Technology* **24**, 243–254. Light scattering by rough surfaces: electromagnetic model for lighting simulations.
9. E. I. Thorsos 1988 *Journal of the Acoustical Society of America* **83**, 78–92. The validity of the Kirchhoff approximation for rough surface scattering using a Gaussian roughness spectrum.
10. K. A. O'Donnell and E. R. Mendez 1987 *Journal of Optical Society of America A* **4**, 1194–1205. Experimental study of scattering from characterized random surfaces.
11. A. Wirgin 1989 *Journal of the Acoustical Society of America* **85**, 670–679. Scattering from hard and soft corrugated surfaces: iterative corrections to the Kirchoff approximation through the extinction theorem.
12. C. Macaskill 1991 *Journal of Optical Society of America A* **8**, 88–96. Geometric optics and enhanced backscatter from very rough surfaces.
13. S. T. McDaniel and A. D. Gorman 1983 *Journal of the Acoustical Society of America* **73**, 1476–1486. An examination of the composite-roughness scattering model.
14. J. M. Soto-Crespo and M. Nieto-Vesperinas 1989 *Journal of Optical Society of America A* **6**, 367–384. Electromagnetic scattering from very rough random surfaces and deep reflection gratings.
15. C. Eftimiu 1990 *Journal of Optical Society of America A* **7**, 875–884. Scattering by a rough dielectric interface: a modified Wiener–Hermite expansion approach.
16. J. M. Soto-Crespo and M. Nieto-Vesperinas 1990 *Journal of Optical Society of America A* **7**, 1185–1201. Scattering from slightly rough random surfaces: a detailed study on the validity of the small perturbation method.

17. C. MACASKILL and B. J. KACHOYAN 1988 *Journal of the Acoustical Society of America* **84**, 1826–1835. Numerical evaluation of the statistics of acoustic scattering from a rough surface.
18. A. G. VORONOVICH 1996 *Waves in Random Media* **6**, 151–167. Non-local small-slope approximation for wave scattering from rough surfaces.
19. S. L. BROSCHAT and E. I. THORSOS 1997 *Journal of the Acoustical Society of America* **101**, 2615–2625. An investigation of the small slope approximation for scattering from rough surfaces. Part II. Numerical studies.
20. D. M. MILDER 1996 *Journal of the Acoustical Society of America* **100**, 759–768. Role of the admittance operator in rough-surface scattering.
21. R. J. WAGNER 1966 *Journal of the Acoustical Society of America* **41**, 138–147. Shadowing of randomly rough surfaces.
22. D. F. MCCAMMON and S. T. MCDANIEL 1986 *Journal of the Acoustical Society of America* **79**, 1778–1785. Surface velocity, shadowing, multiple scattering and curvature on a sinusoid.
23. L. TSANG, C. H. CHAN and K. PAK 1994 *Journal of Optical Society of America A* **11**, 711–715. Backscattering enhancement of a two-dimensional random rough surface (three-dimensional scattering) based on Monte Carlo simulations.
24. M. J. KIM, J. C. DAINTY, A. T. FRIBERG and A. J. SANT 1990 *Journal of Optical Society of America A* **7**, 569–577. Experimental study of enhanced backscattering from one- and two-dimensional random surfaces.

APPENDIX A

Consider equation (9) which expresses the total number of sound rays reflected in the same direction $\mathbf{k}_2$. All these rays are reflected by surface elements having the same normal vector $\mathbf{n}$. This vector can also be expressed by the vectorial difference between $\mathbf{k}_2$ and $\mathbf{k}_1$, which yields

$$\mathbf{n} = \frac{1}{\sqrt{1+|\boldsymbol{\gamma}|^2}}(-\gamma_x, -\gamma_y, 1) = \frac{1}{2|\cos\theta_s|}(\sin\theta_2\cos\phi_2 - \sin\theta_1, \sin\theta_2\sin\phi_2, \cos\theta_2 + \cos\theta_1). \tag{A1}$$

From this equation, the relations between (θ_2, ϕ_2) and (γ_x, γ_y) can be derived:

$$\gamma_x = \frac{\sin\theta_1 - \sin\theta_2\cos\phi_2}{\cos\theta_2 + \cos\theta_1}, \qquad \gamma_y = \frac{-\sin\theta_2\sin\phi_2}{\cos\theta_2 + \cos\theta_1}. \tag{A2}$$

The denominator must be positive, just as the z-component of the normal vector. The relations (A2) express that for each value of θ_2 in $[0, \pi - \theta_1[$ and each value of ϕ_2 in $[0, 2\pi[$, there exists only one pair of values (γ_x, γ_y). These relations can be inverted, which gives the following:

$$\cos\theta_2 = -\cos\theta_1 + 2\frac{\gamma_x\sin\theta_1 + \cos\theta_1}{1+|\boldsymbol{\gamma}|^2},$$

$$\cot\phi_2 = \frac{1}{2\gamma_y}\frac{2\gamma_x\cos\theta_1 - \sin\theta_1(1-\gamma_x^2+\gamma_y^2)}{\gamma_x\sin\theta_1 + \cos\theta_1},$$

$$\operatorname{sign}(\sin\phi_2) = -\operatorname{sign}(\gamma_y). \tag{A3}$$

Care must be taken for some specific values of (γ_x, γ_y). For example, the pair $\gamma_x = \sin\theta_1/(1+\cos\theta_1)$ and $\gamma_y = 0$ leads to $\theta_2 = 0$ and an undetermined value of ϕ_2. In fact, if the relationship between both pairs of variables (A3) is more deeply analyzed, the following conclusions can be drawn:

—there is a one-to-one relation between both pairs of variables if $(\gamma_x > -\cot\theta_1, -\infty < \gamma_y < +\infty)$ and $(0 \leqslant \theta_2 < \pi - \theta_1, 0 \leqslant \phi_2 < 2\pi)$,
—except for the pair $\gamma_x = \sin\theta_1/(1+\cos\theta_1)$ and $\gamma_y = 0$ (the case already mentioned above) and
—except for $\theta_2 = \pi - \theta_1$ and $\phi_2 = 0$, leading to $\gamma_x = -\cot\theta_1$ and an undetermined value of γ_y.

This last case need not be considered, since the value $(\theta_2 = \pi - \theta_1)$ has been explicitly excluded.

The element of solid angle $\mathrm{d}\Omega$ is defined by $(\theta_2 \leqslant t \leqslant \theta_2 + \mathrm{d}\theta_2, \phi_2 \leqslant f \leqslant \phi_2 + \mathrm{d}\phi_2)$. In the domain where there is a one-to-one correspondence between both pairs of variables, it is associated with a domain $D(\boldsymbol{\gamma})$ of the variables (γ_x, γ_y), such that

$$\mathrm{size}\{D(\boldsymbol{\gamma})\} = \frac{\partial\gamma_x\gamma_y}{\partial\theta_2\phi_2}\,\mathrm{d}\theta_2\,\mathrm{d}\phi_2 = \frac{\mathrm{d}\Omega}{2\cos^2\alpha(\cos\theta_2 + \cos\theta_1)} \tag{A4}$$

with the angle α defined in equation (5).

Around $\theta_2 = 0$, care must be taken because the one-to-one relationship between (θ_2, ϕ_2) and (γ_x, γ_y) fails. The element of solid angle $\mathrm{d}\Omega$ is defined here by $(0 \leqslant t \leqslant \mathrm{d}\theta_2,\ 0 \leqslant f < 2\pi)$. The corresponding domain $D(\boldsymbol{\gamma})$ is expressed by the replacement of (θ_2, ϕ_2) by (t, f) in equation (A2) and, considering that t is a small value $(\cos t \sim 1)$:

$$\gamma_x = \frac{\sin\theta_1}{1+\cos\theta_1} - \frac{t\cos f}{1+\cos\theta_1}, \quad \gamma_y = -\frac{t\sin f}{1+\cos\theta_1} \quad (0 \leqslant t \leqslant \mathrm{d}\theta_2,\ 0 \leqslant f < 2\pi), \tag{A5}$$

This is the equation of a circular domain, centered at $\gamma_x = \sin\theta_1/(1+\cos\theta_1)$ and $\gamma_y = 0$, with a radius equal to $(\mathrm{d}\theta_2/(1+\cos\theta_1))$. Therefore, the size of this domain $D(\boldsymbol{\gamma})$ is simply given by

$$\mathrm{size}\{D(\boldsymbol{\gamma})\} = \pi\left(\frac{\mathrm{d}\theta_2}{1+\cos\theta_1}\right)^2. \tag{A6}$$

Finally, considering that $\mathrm{d}\Omega = \pi(\mathrm{d}\theta_2)^2$ in equation (A6), the expression (A4) is also valid in this case.

APPENDIX B

From the definition of $\eta(\theta_2, \phi_2)$ in equation (20), the following expression is derived for isotropic surfaces:

$$\eta(\theta_2)^{-1} = \sin\theta_2 \int_{|\cot\theta_2|}^{+\infty} uW(u)\,\mathrm{d}u - \cos\theta_2 \int_{\cot\theta_2}^{+\infty} W(u)\,\mathrm{d}u,$$

$$W(u) = \int_{-\infty}^{+\infty} w(u\cos\phi_2 - v\sin\phi_2; u\sin\phi_2 + v\cos\phi_2)\,\mathrm{d}v. \tag{B1}$$

For isotropic surfaces, it can be shown that $W(u) = W(-u)$, which allows taking the absolute value of $\cot\theta_2$ as the lower bound of the first integral. If $\theta_2 > \pi/2$, $\alpha_w(\pi - \theta_2)$ can be derived from equation (11):

$$\alpha_w(\pi - \theta_2)^{-1} = \int_{\cot\theta_2}^{+\infty} (\gamma_x|\tan\theta_2| + 1)\,\mathrm{d}\gamma_x \int_{-\infty}^{+\infty} w(\gamma_x, \gamma_y)\,\mathrm{d}\gamma_y. \tag{B2}$$

Again, for isotropic surfaces, the last integral gives $W(\gamma_x)$ and, comparing equations (B1) and (B2) leads to

$$\eta(\theta_2)^{-1} = |\cos\theta_2|\,\alpha_w(\pi - \theta_2)^{-1}, \quad \theta_2 > \pi/2. \tag{B3}$$

If $\theta_2 \leqslant \pi/2$, the following expression of $\alpha_w(\theta_2)$ is derived from equation (11):

$$\alpha_w(\theta_2)^{-1} = \tan\theta_2 \int_{-\cot\theta_2}^{+\infty} \gamma_x W(\gamma_x)\,\mathrm{d}\gamma_x + \int_{-\cot\theta_2}^{+\infty} W(\gamma_x)\,\mathrm{d}\gamma_x. \tag{B4}$$

As $W(\gamma_x) = W(-\gamma_x)$ for isotropic surfaces, the lower bound of the first integral can be replaced by $|\cot\theta_2|$. Furthermore, the last integral is equal to $(1 - \int_{\cot\theta_2}^{+\infty})$, since $w(\gamma_x, \gamma_y)$ is a p.d.f.:

$$\eta(\theta_2)^{-1} = \cos\theta_2(\alpha_w(\theta_2)^{-1} - 1), \quad \theta_2 \leqslant \pi/2. \tag{B5}$$

Finally, recalling that $\alpha_w = 0$ for $\theta_2 > \pi/2$, equations (B3) and (B4) can be used to derive

$$\frac{\eta(\pi - \theta_2)}{\eta(\theta_2)} = \frac{1 - \alpha_w(\theta_2)}{1 - \alpha_w(\pi - \theta_2)}, \quad 0 \leqslant \theta_2 \leqslant \pi. \tag{B6}$$